ENGINEERING TRANSACTIONS • *Engng. Trans.* • 40, 2, 229–248, 1992
Polish Academy of Sciences • Institute of Fundamental Technological Research

FINITE TIMOSHENKO-TYPE BEAM ELEMENT WITH A CRACK

M. KRAWCZUK (GDAŃSK)

The paper presents a method of constructing the stiffness matrix of a Timoshenko-type finite beam element with a single nonpropagating transversal one-edge crack located in the middle of its length. The crack was modelled by adding an additional flexibility matrix to the flexibility matrix of the uncracked element. The terms of the additional matrix were evaluated according to the laws of fracture mechanics. The element was used to perform several numerical tests, the results of which were compared with results of the analytical solutions available in literature. Very good agreement between the presented model and the analytical solution was obtained. The element presented in the paper may be applied to the static and dynamic analysis of many types of structural elements with faults in form of fatigue cracks. The method of formation of the stiffness matrix described in the paper, allows to create finite elements of a beam with various types of cracks (double-edge, circumferential, internal, etc), provided their stress intensity factors are known.

1. INTRODUCTION

Cracks occurring in structural elements of machines lead to local changes in stiffness [1] and alter their dynamic characteristics. This problem was a subject of many papers, the review of which is given by WAUER [2]. First attempts were devoted to the analysis of simple cracked structures such as beams, shafts, frames with a constant cross-section [3-12]. Real structures are more complicated and the analytical methods described in the cited papers are useless. For this reason some of investigators have started to apply FEM for modelling the damaged complex structures. DIRR and SCHMALHORST [13] applied for modelling cracked shafts, 3-D, 20-node isoparametric finite elements. The crack was modelled by separating the nodes on both sides of the crack. A similar model was applied by OSTACHOWICZ and KRAWCZUK [14-15] in papers devoted to the dynamic analysis of cracked beams and turbine blades. SHEN and PIERRE [16] applied the 2-D isoparametric finite elements with the singular shape function for the analysis of natural vibrations of the beams with double-edge cracks.

Other authors use the finite elements with cracks [17-20] for static and dynamic analysis. In the case of a beam finite element, the Bernoulli-Euler theory was applied. HAISTY and SPRINGER [17] elaborated the finite beam element with an open double-edge crack. The crack was modelled by springs, the stiffness of which was calculated by comparing the strain energy of the springs with the corresponding stress intensity factors. QIAN [18] and GOUNARIS [19] modelled the crack in a beam by additional compliances, the values of which were calculated on the basis of fracture mechanics. The method of constructing the stiffness matrix for the rectangular plate finite element with an internal open crack was described by QIAN [20]. In this case, the Kirchhoff-Love theory was applied.

The main purpose of the present paper is to design the finite beam element with an open one-edge crack. The model of the element should account for the effects of shear deformation (Timoshenko beam). The element can be used for static and dynamic analysis of cracked beams, shafts, frames and columns. In the order to verify the presented model, the numerical calculations were carried out. The results of numerical investigations were compared with the analytical solutions and experimental data.

2. CONSTRUCTION OF THE STIFFNESS MATRIX OF CRACKED, TIMOSHENKO-TYPE BEAM FINITE ELEMENT

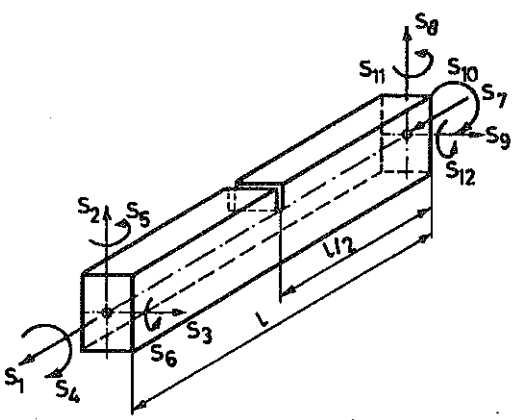

FIG. 1. Cracked beam finite element with two nodes and six degrees of freedom at the node.

The finite-beam element with two nodes and six degrees of freedom at the node is presented in Fig.1. Taking into account that the stress field is affected only in the region adjacent to the crack (principle of Saint-Venant), the strain energy of the element U is

$$U = U^0 + U^1, \tag{2.1}$$

where U^0 is the strain energy of the element without a crack, U^1 is the additional strain energy due to the crack.

The strain energy of the uncracked element U^0 is

$$U^0 = \int_0^l \frac{N^2 dx}{2EA} + \int_0^l \frac{M_y^2 dx}{2EJ_y} + \int_0^l \frac{M_z^2 dx}{2EJ_z} + \int_0^l \frac{M_s^2 dx}{2GJ_0} + \int_0^l \frac{\beta_y P_y^2 dx}{2GA} + \int_0^l \frac{\beta_z P_z^2 dx}{2GA}, \tag{2.2}$$

where l is the length of the element, N is the axial force, M_y, M_z are the bending moments, M_s is the torsional moment, P_y, P_z are the shear forces, E is Young's modulus, G is shear modulus, A is the area of the cross-section of the element, J_y, J_z are the geometrical moments of inertia of the cross-section of the element, J_0 is the polar moment of inertia of the cross-section of the element, β_y, β_z are the shear coefficients of the cross-section of the element (for typical shapes of the cross-section the values of the shear coefficients are given in [21]).

Inserting the following relationships (see Fig.1):

$$\begin{aligned} N &= S_1, & M_s &= S_4, \\ M_y &= S_5 + S_3 l, & M_z &= S_6 + S_2 l, \\ P_y &= S_2, & P_z &= S_5, \end{aligned} \tag{2.3}$$

into (2.2) and integrating with respect to the length of the element, the strain energy of the uncracked element is

$$U^0 = \frac{S_1^2 l}{2EA} + \frac{S_5^2 l}{2EJ_y} + \frac{S_5 S_3 l}{2EJ_y} + \frac{S_3^2 l^3}{6EJ_y} + \frac{S_6^2 l}{2EJ_z} + \frac{S_6 S_2 l}{2EJ_z} + \frac{S_2^2 l^3}{6EJ_z} + \frac{S_4^2 l}{2GJ_0} + \frac{\beta_z S_2^2 l}{2GA} + \frac{\beta_y S_3^2 l}{2GA}. \tag{2.4}$$

The additional strain energy U^1 due to the crack [22]

$$U^1 = \frac{1}{E'} \int_F \left[\sum_{i=1}^{i=6} K_{\mathrm{I}i}^2 + \sum_{i=1}^{i=6} K_{\mathrm{II}i}^2 + (1+\nu) \sum_{i=1}^{i=6} K_{\mathrm{III}i}^2 \right] dF, \tag{2.5}$$

where $E' = E$ for plane stress, $E' = E/(1-\nu)^2$ for plane strain, ν is Poisson's ratio, F is the area of the crack, $K_{\mathrm{I}i}$, $K_{\mathrm{II}i}$, $K_{\mathrm{III}i}$ are the stress intensity factors corresponding to three modes of crack deformation [22] (nonzero stress intensity factors for circular and rectangular cross-sections, the dimensions of which are given in Fig.2, are presented in Appendix 1).

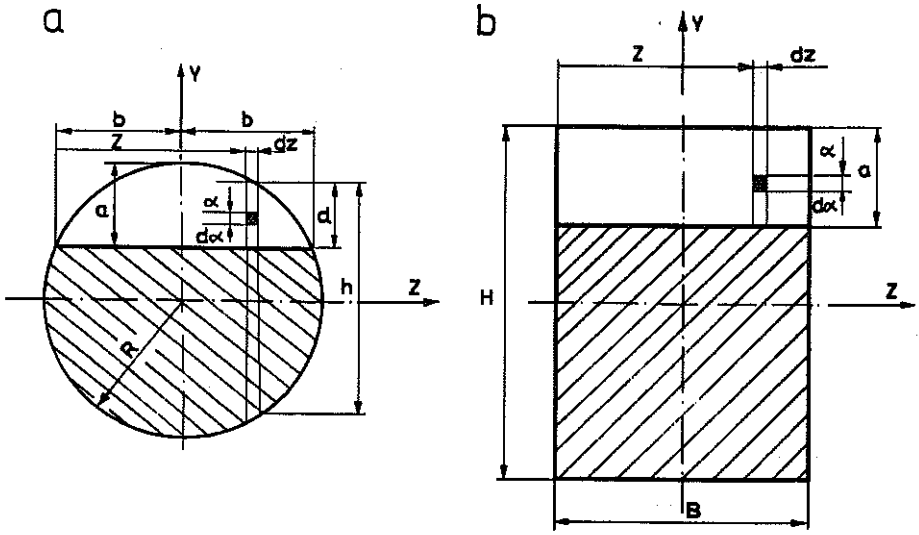

FIG. 2. Cross-sections of the finite element at the crack.

The flexibility coefficient of the cracked beam finite element c_{ij} is a sum of the flexibility coefficient of the uncracked element c_{ij}^0, and the additional flexibility coefficient due to the crack c_{ij}^1

$$c_{ij} = c_{ij}^0 + c_{ij}^1, \qquad i = 1,6; \quad j = 1,6, \tag{2.6}$$

where

$$c_{ij}^0 = \partial^2 U^0 / \partial S_i \partial S_j \qquad c_{ij}^1 = \partial^2 U^1 / \partial S_i \partial S_j.$$

Taking into account relations (2.4), (2.5) and (2.6), the flexibility coefficients c_{ij}^0, c_{ij}^1 are obtained. The coefficients are used to construct the stiffness matrix of the element.

The flexibility matrix of the uncracked beam finite element takes the form

$$\text{(2.7)}\quad \mathbf{C}^0 = \begin{bmatrix} \frac{l}{EA} & 0 & 0 & 0 & 0 & 0 \\ 0 & \frac{l^3}{3EJ_z} + \frac{\beta_z l}{GA} & 0 & 0 & 0 & \frac{l^2}{2EJ_z} \\ 0 & 0 & \frac{l^3}{3EJ_y} + \frac{\beta_y l}{GA} & 0 & \frac{l^2}{2EJ_y} & 0 \\ 0 & 0 & 0 & \frac{l}{GJ_0} & 0 & 0 \\ 0 & 0 & \frac{l^2}{2EJ_y} & 0 & \frac{l}{EJ_y} & 0 \\ 0 & \frac{l^2}{2EJ_z} & 0 & 0 & 0 & \frac{l}{EJ_z} \end{bmatrix},$$

and the matrix of the additional flexibilities can be written in the form

$$\text{(2.8)}\quad \mathbf{C}^1 = \begin{bmatrix} c_{11} & 0 & 0 & 0 & c_{15} & c_{16} \\ 0 & c_{22} & 0 & c_{24} & 0 & 0 \\ 0 & 0 & c_{33} & c_{34} & 0 & 0 \\ 0 & c_{42} & c_{43} & c_{44} & 0 & 0 \\ c_{51} & 0 & 0 & 0 & c_{55} & c_{56} \\ c_{61} & 0 & 0 & 0 & c_{65} & c_{66} \end{bmatrix}.$$

The relations used for calculating the terms of the additional flexibility matrix $\mathbf{C}^1$ in the case of circular and rectangular cross-sections are presented in Appendix 2 and 3. The graphs of the dimensionless flexibilities $\bar{c}_{ij}$ at the crack for the circular and the rectangular cross-sections are presented in Fig.3 and 4. Having derived the flexibility matrix of the cracked finite element and taking the principle of virtual work into account, the stiffness matrix of the element can be written in the form

$$\text{(2.9)}\quad \mathbf{K}_c = \mathbf{T}^T \mathbf{C}^{-1} \mathbf{T},$$

where $\mathbf{C} = \mathbf{C}^0 + \mathbf{C}^1$, $\mathbf{T}$ – the matrix obtained from the statical equilibrium conditions of the element, assuming that the crack is located in the middle

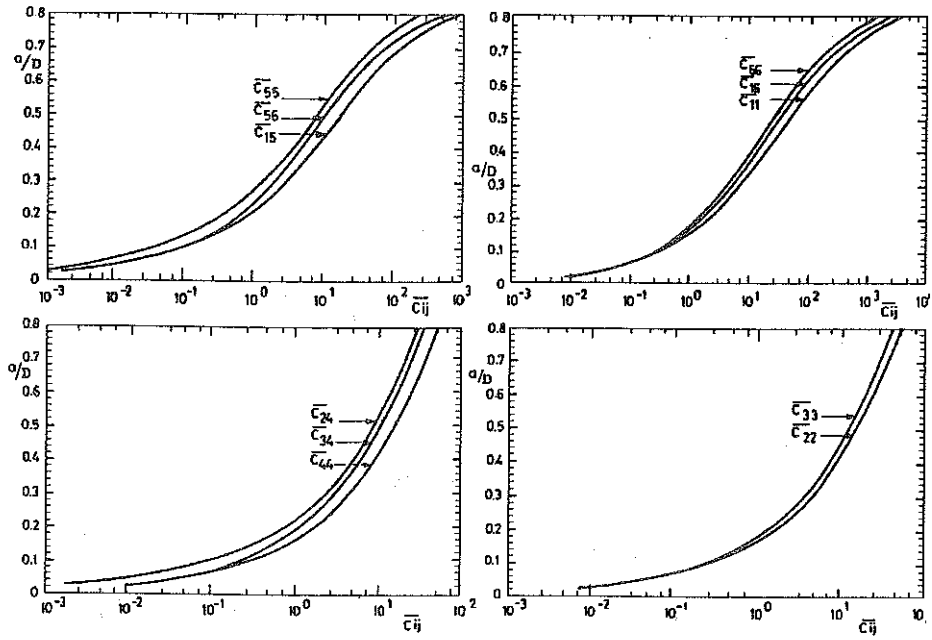

FIG. 3. Nondimensional flexibility coefficients for finite beam element of circular cross-section due to the crack.

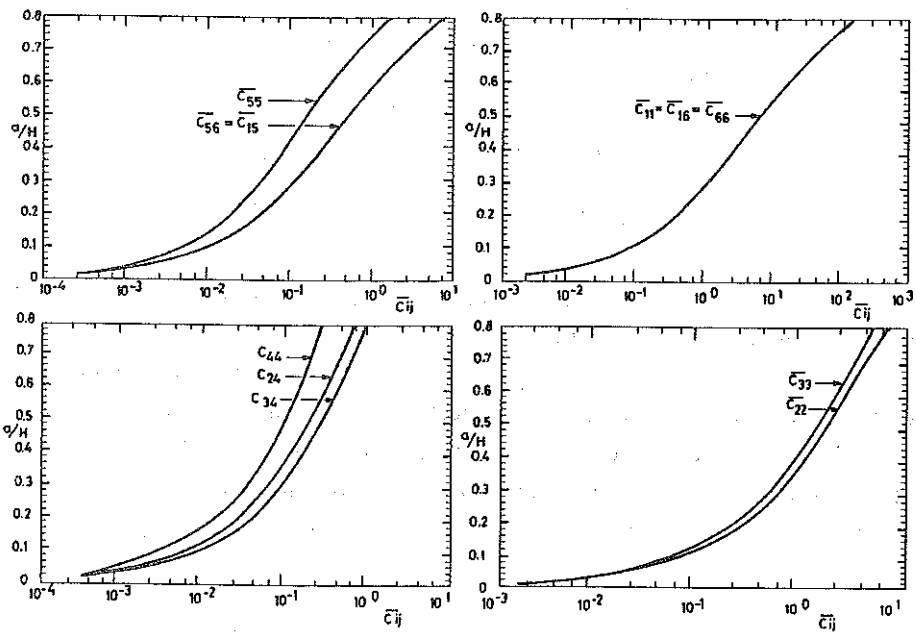

FIG. 4. Nondimensional flexibility coefficients for finite beam element of rectangular cross-section due to the crack.

of the element,

$$\mathbf{T} = \begin{bmatrix} -1 & 0 & 0 & 0 & 0 & 0 \\ 0 & -1 & 0 & 0 & 0 & 0 \\ 0 & 0 & -1 & 0 & 0 & 0 \\ 0 & 0 & 0 & -1 & 0 & 0 \\ 0 & 0 & -l & 0 & -1 & 0 \\ 0 & -l & 0 & 0 & 0 & -1 \\ 1 & 0 & 0 & 0 & 0 & 0 \\ 0 & 1 & 0 & 0 & 0 & 0 \\ 0 & 0 & 1 & 0 & 0 & 0 \\ 0 & 0 & 0 & 1 & 0 & 0 \\ 0 & 0 & 0 & 0 & 1 & 0 \\ 0 & 0 & 0 & 0 & 0 & 1 \end{bmatrix}. \tag{2.10}$$

In case when the terms of the flexibility matrix due to the crack are neglected, we obtain the stiffness matrix identical with Przemieniecki's matrix [23] (assuming that the coefficients β_y, β_z correspond to the ratio A/A_s in Przemieniecki's matrix). In the case when coefficients $\beta_y = \beta_z = 0$ we obtain the stiffness matrix identical to Bernoulli-Euler's beam finite element.

The method of formation of the stiffness matrix described in the paper may be used to construct finite beam elements with various types of cracks (double-edge, circumferential, internal, etc.), provided their stress intensity factors are known.

3. Numerical tests

The numerical calculations were carried out in order to verify the presented model of the finite element. The results of numerical investigations were compared with analytical solutions and experimental data. The inertia matrix was assumed in the same form as for the uncracked Timoshenko beam finite element [23].

3.1. Natural vibrations

Natural vibrations of the linear elastic body, discretized by FEM (damping and preloads being disregarded) are described by the well-known equation [26]:

$$\mathbf{M}\ddot{\bar{q}} + \mathbf{K}\bar{q} = \mathbf{0}, \tag{3.1}$$

where M is the global matrix of inertia, K is the global matrix of stiffness, and $\ddot{\bar{q}}$, $\bar{q}$ are the global column matrices of generalized accelerations and displacements.

In order to determine the natural frequency of vibrations, the Eq.(3.1) should be transformed to the standard form [26]. In the present paper the standard form of Eq.(3.1) was solved by the QL-method [27].

Test 1

For a cantilever beam of circular cross-section, the influence of coupled bending and torsional vibrations due to the crack of the first natural bending frequency was analyzed. The calculations were carried out for various ratios of the beam radius R to the beam length l, and for various one-edge crack depths a/D, at a constant position of the crack $l_1/l = 0.2$. The beam was discretized by 10 finite elements of Timoshenko-type beam. The beam was

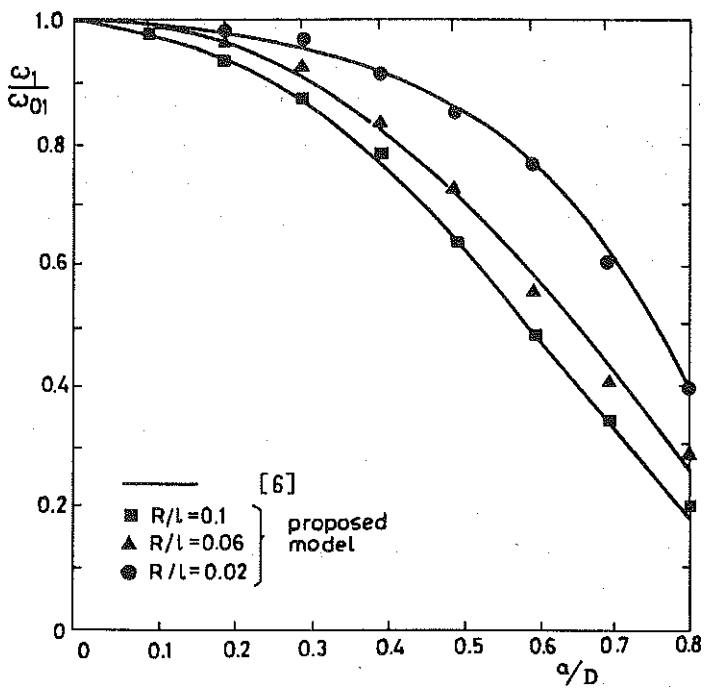

FIG. 5. Relative changes of the first natural bending frequency of a cantilever Timoshenko beam as a function of relative depth of the crack a/D and slenderness ratio R/l. The crack position is $l_1/l = 0.2$ (ω_{01} is the first natural bending frequency of the uncracked beam).

made from steel of the following properties: $E = 2.1 \times 10^{11}$ N/m^2, $G = 8.07 \times 10^{10}$ N/m^2, $\rho = 7860$ kg/m^3, $\nu = 0.3$. The results obtained were compared with the results of the analytical calculations given by PAPADOPOULOS and DIMAROGONAS [6] – Fig.5.

Next the analysis of the effect of one-edge crack depth a/D and its position on the variation of the first natural frequency of bending for the beam with constant ratio $R/l = 0.0125$ was performed. The obtained results, presented in Fig.6, are compared with results of the analytical solution given in [6].

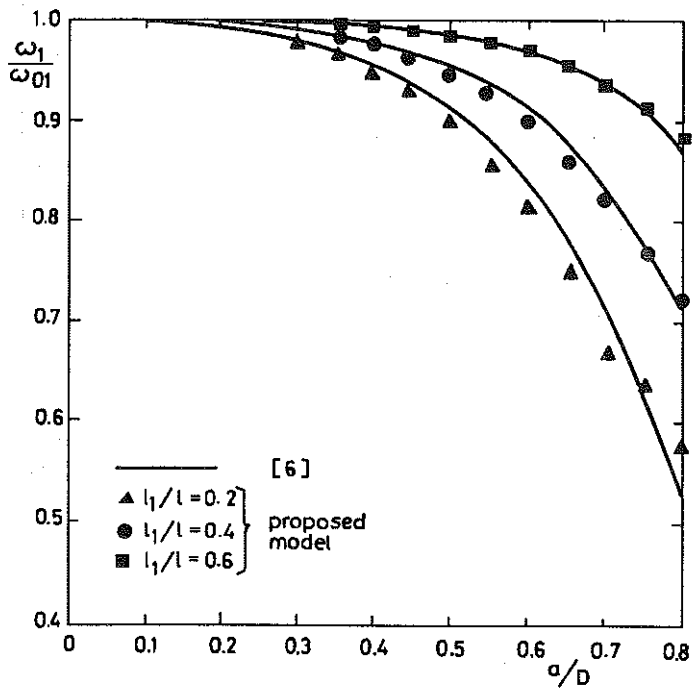

FIG. 6. Relative changes of the first natural bending frequency of a cantilever Timoshenko beam as a function of relative depth a/D and relative position l_1/l of the crack. The slenderness ratio is $R/l = 0.0125$.

Test 2

For a simply supported beam of circular cross-section ($R/l = 0.1$), the variation of the first natural bending frequency for various one-edge crack depths a/D and positions l_1 were calculated. The material characteristics and discretization method were assumed as in Test 1. The results of calculations, compared with the analytical results given by RAJAB and AL-

SABEEH [7], are presented in Fig.7.

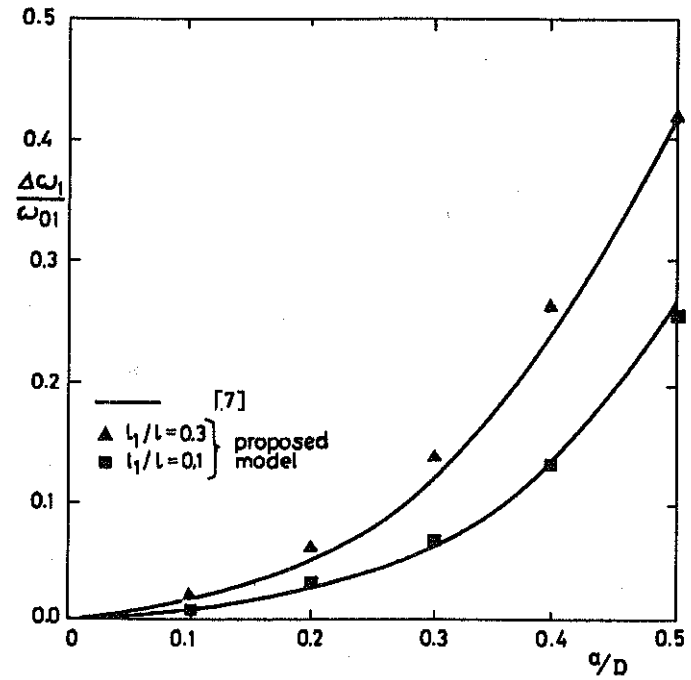

FIG. 7. Relative changes of the first natural bending frequency of simple supported Timoshenko beam as a function of relative depth a/D and relative position l_1/l of the crack. The slenderness ratio is $R/l = 0.1$.

Test 3

For a cantilever beam of rectangular cross-section $B \times H = 0.01 \times 0.02$ m and length $l = 0.4$ m, the changes in the first natural bending frequency for various one-edge crack depths a/H and constant position $l_1/l = 0.2$ were calculated. The obtained results were compared with the analytical results (for a Bernoulli-Euler beam) and with the experimental data [24] – Fig.8.

Next, for the same beam, the influence of two one-edge cracks on the variation of the first natural bending frequency was analyzed. The same depths of the crack $a_1/H = a_2/H = 0.5$ and constant position of the first crack $l_1/l = 0.05$ were assumed. The position of the second crack l_2/l was varied. The results obtained were compared with results of the analytical calculations (for a Bernoulli-Euler beam) and with the experimental data [24] – Fig.9.

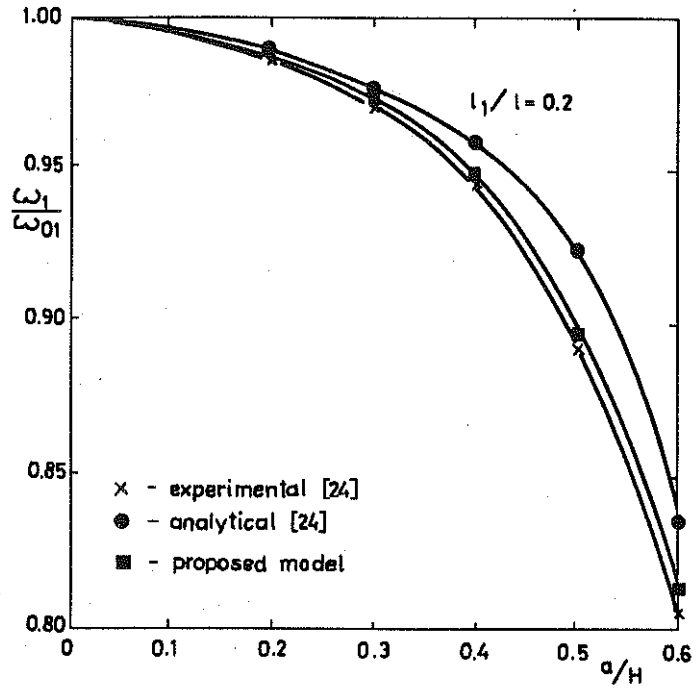

FIG. 8. Relative changes of the first natural bending frequency of a cantilever beam as a function of relative depth a/H. The crack position is $l_1/l = 0.2$.

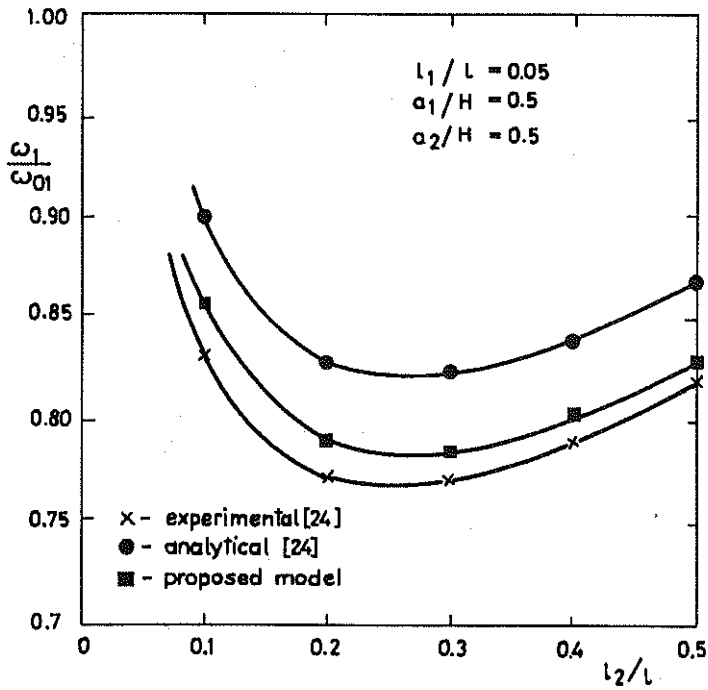

FIG. 9. Relative changes of the first natural bending frequency of a cantilever beam with two cracks as a function of relative position of the second crack l_2/l.

3.2. Forced vibrations

Forced vibrations of the linear elastic body, discretized by FEM (neglecting the damping and preloads) are described by the well-known equation [26]

$$\mathbf{M}\ddot{\bar{q}} + \mathbf{K}\bar{q} = P(t), \tag{3.2}$$

where $P(t)$ is the global column matrix of the excitation forces.

In the case of harmonic excitation, Eq.(3.2) can be transformed to a system of algebraic equations, the roots of which are the vibration amplitudes. In the present paper the system of algebraic equations was solved by the Gauss elimination method [27].

Test 4

For the cantilever beam of circular cross-section $D = 0.064$ m and length $l = 0.8$ m, the amplitudes of the bending and longitudinal vibrations were calculated. The free end of the beam was subjected to harmonically variable axial force, the amplitude of which was equal 100 N. The frequency of the

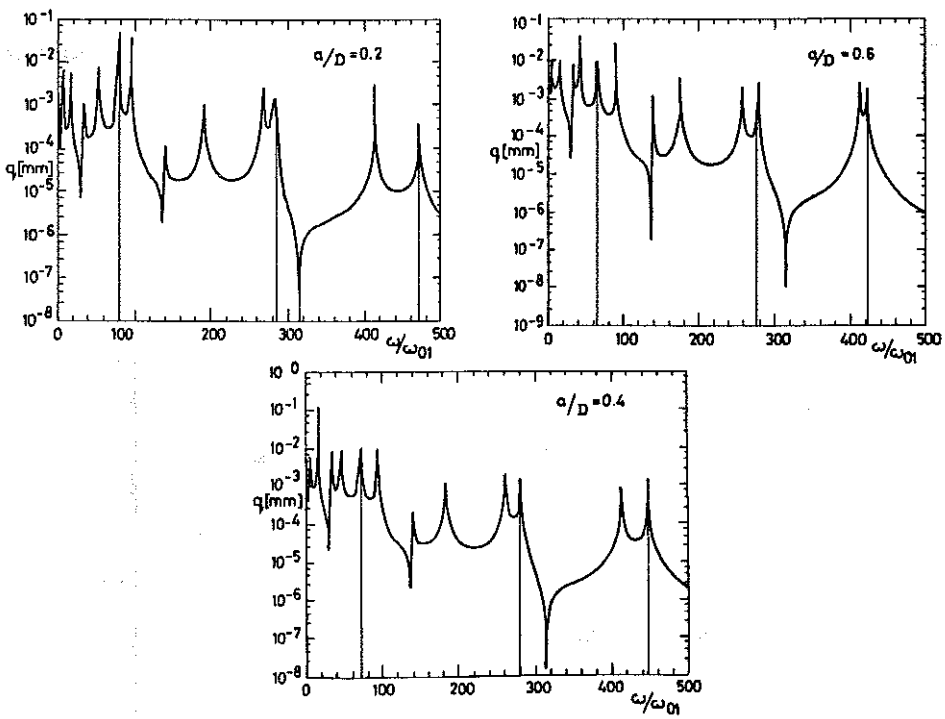

FIG. 10. Coupled bending vibrations for several crack depths. The crack position is $l_1/l = 0.3$.

excitation force was changing from 0 to 500 ω_{01} (where ω_{01} is the first natural bending frequency of the uncracked beam). The material data and discretization of the beam were assumed as in Test 1. The obtained spectrum of amplitudes of the bending and longitudinal vibrations of the beam end for various depths of the one-edge crack a/D, and at the constant position $l_1/l = 0.3$, is presented in Figs.10–11. The crack produces additional resonant frequencies (corresponding the natural bending frequencies) in the spectrum of the longitudinal vibrations. Additional resonant frequencies also appeared in the spectrum of the bending vibration. Similar results were obtained analytically by PAPADOPOULOS and DIMAROGONAS [4].

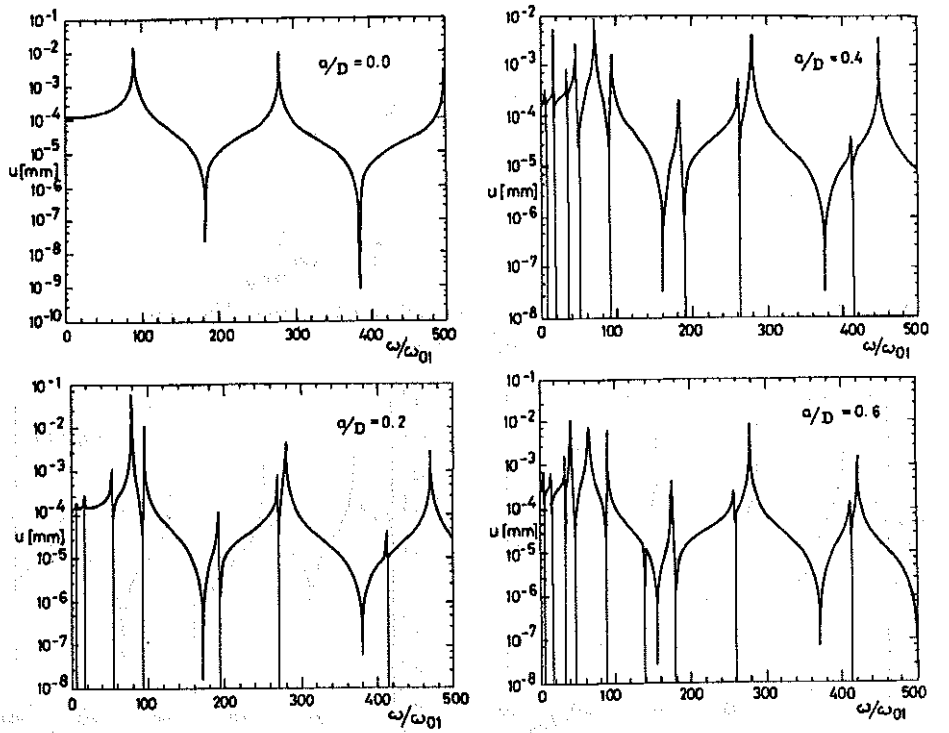

FIG. 11. Coupled longitudinal vibrations for several crack depths. The crack position is $l_1/l = 0.3$.

Test 5

For a cantilever beam of circular cross-section $D = 0.064$ m and length $l = 0.8$ m, the amplitudes of torsional and bending vibrations were calculated. The free end of the beam was subjected to harmonically variable torsional moment, the amplitude of which was equal to 100 Nm. Frequency

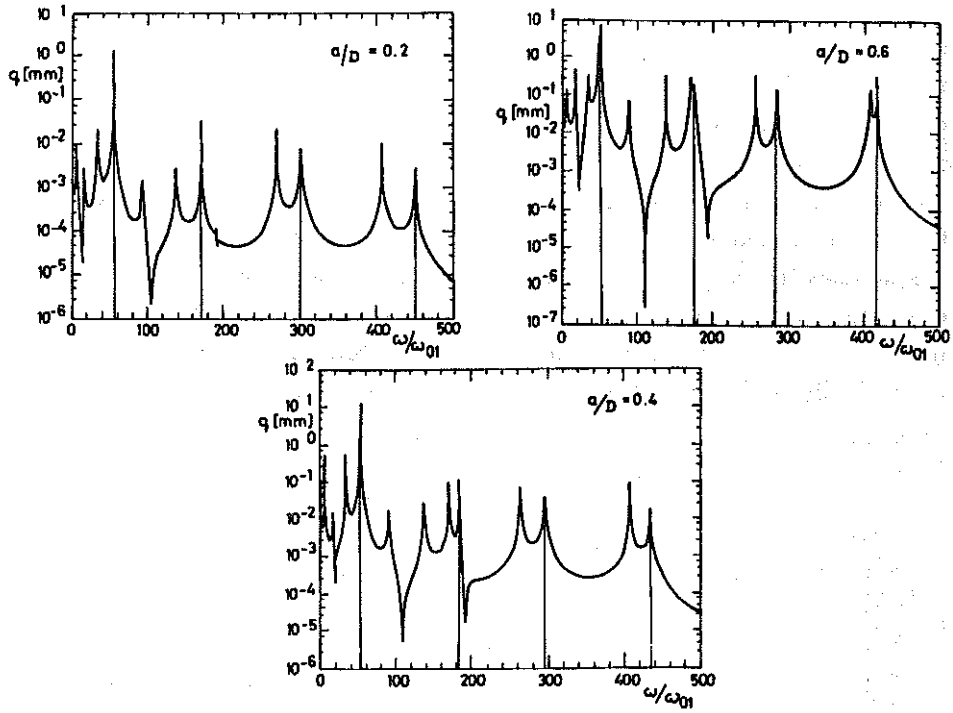

FIG. 12. Coupled bending vibrations for several crack depths. The crack position is $l_1/l = 0.3$.

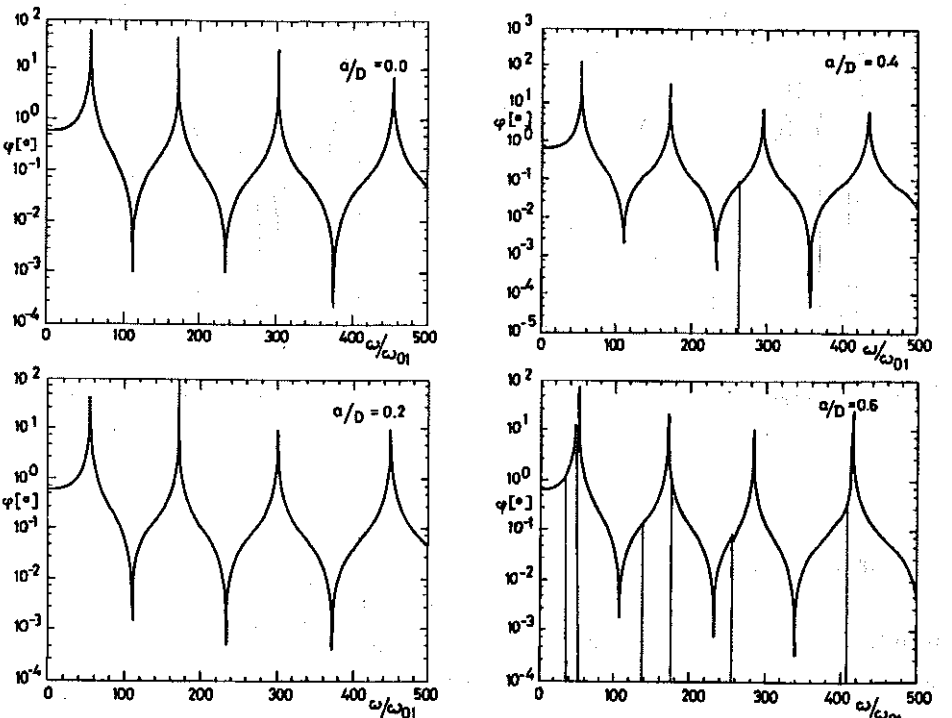

FIG. 13. Coupled torsional vibrations for several crack depths. The crack position is $l_1/l = 0.3$.

of the excitation moment was varied from 0 to 500 ω_{01} (where ω_{01} is the first natural bending frequency of an uncracked beam). The material data and discretization pattern of the beam were assumed as in Test 1. The obtained spectrum of amplitudes of the bending and torsional vibrations of the beam end for various depths of the edge crack a/D and at constant position $l_1/l = 0.3$ is presented in Figs.12–13. The crack produces additional resonant frequencies (corresponding to the natural bending frequencies) in the spectrum of torsional vibrations. Additional resonant frequencies also appeared in the spectrum of the bending vibration. Similar results were obtained analytically by PAPADOPOULOS and DIMAROGONAS [5].

4. CONCLUSIONS

The paper presents a method of calculating the stiffness matrix of the Timoshenko-type finite beam element with an open nonpropagating one-edge crack. The method described in the paper allows to design finite beam elements containing other types of cracks (double-edge, circumferential, internal, etc) if their stress intensity factors are known. Results of the numerical tests prove that this element may be used for dynamic analysis of cracked structures. Very good agreement between the results of numerical investigations and the analytical solutions and also the experimental data was obtained. The described element may be used for the static and dynamic analysis of beams, frames, shafts and columns with cracks.

APPENDIX 1

Nonzero stress intensity factors for circular and rectangular cross-sections:

K_{ij}	circular cross-section	rectangular cross-section
$K_{\mathrm{I}1}$	$\frac{S_1}{\Pi R^2}\sqrt{\Pi\alpha}\,F_1(\alpha/h)$	$\frac{S_1}{BH}\sqrt{\Pi\alpha}\,F_1(\alpha/H)$
$K_{\mathrm{I}5}$	$\frac{4S_5 z}{\Pi R^4}\sqrt{\Pi\alpha}\,F_2(\alpha/h)$	$\frac{12S_5 z}{HB^3}\sqrt{\Pi\alpha}\,F_2(\alpha/H)$
$K_{\mathrm{I}6}$	$\frac{4S_6}{\Pi R^4}\sqrt{R^2-z^2}\sqrt{\Pi\alpha}\,F_1(\alpha/h)$	$\frac{6S_6}{BH^2}\sqrt{\Pi\alpha}\,F_1(\alpha/H)$
$K_{\mathrm{II}2}$	$\frac{\beta_z S_2}{\Pi R^2}\sqrt{\Pi\alpha}\,F_{\mathrm{II}}(\alpha/h)$	$\frac{\beta_z S_2}{BH}\sqrt{\Pi\alpha}\,F_{\mathrm{II}}(\alpha/H)$

K_{ij}	circular cross-section	rectangular cross-section
K_{II4}	$\frac{2S_4 z}{\Pi R^4}\sqrt{\Pi\alpha}\,F_{II}(\alpha/h)$	$S_4\Phi_y\sqrt{\Pi\alpha}\,F_2(\alpha/H)$
K_{III3}	$\frac{\beta_y S_3}{\Pi R^2}\sqrt{\Pi\alpha}\,F_{III}(\alpha/h)$	$\frac{\beta_y S_3}{BH}\sqrt{\Pi\alpha}\,F_{III}(\alpha/H)$
K_{III4}	$\frac{2S_4}{\Pi R^4}\sqrt{R^2-z^2}\sqrt{\Pi\alpha}\,F_{III}(\alpha/h)$	$S_4\Phi_z\sqrt{\Pi\alpha}\,F_{III}(\alpha/H)$

where: Φ_y, Φ_z – functions describing the distribution of stresses during torsion of the rectangular cross-section [25].

The correction functions assuming finite dimension of a circular cross-section [4] have the form

$$
\begin{aligned}
F_1 &= \sqrt{\tan\lambda/\lambda}\left[0.752 + 2.02(\alpha/h) + 0.37(1-\sin\lambda)^3\right]/\cos\lambda\,,\\
F_2 &= \sqrt{\tan\lambda/\lambda}\left[0.923 + 0.199(1-\sin\lambda)^4\right]/\cos\lambda\,,\\
F_{II} &= \left[1.122 - 0.561(\alpha/h) + 0.085(\alpha/h)^2 + 0.18(\alpha/h)^3\right]/\sqrt{1-\alpha/h}\,,\\
F_{III} &= \sqrt{\tan\lambda/\lambda} \qquad \text{where} \quad \lambda = \Pi\alpha/2h\,,
\end{aligned}
$$

and for a rectangular cross-section [5],

$$
\begin{aligned}
F_1 &= \sqrt{\tan\lambda/\lambda}\left[0.752 + 2.02(\alpha/h) + 0.37(1-\sin\lambda)^3\right]/\cos\lambda\,,\\
F_2 &= \sqrt{\tan\lambda/\lambda}\left[0.923 + 0.199(1-\sin\lambda)^4\right]/\cos\lambda\,,\\
F_{II} &= \left[1.30 - 0.65(\alpha/H) + 0.37(\alpha/H)^2 + 0.28(\alpha/H)^3\right]/\sqrt{1-\alpha/H}\,,\\
F_{III} &= \sqrt{\gamma/\sin\gamma} \qquad \text{where} \quad \lambda = \Pi\alpha/2H, \quad \gamma = 2\lambda.
\end{aligned}
$$

Appendix 2

The relations used for calculating the additional flexibility coefficients c^1_{ij} (circular cross-section, plane state of strain):

$c_{11} = \dfrac{4(1-\nu^2)}{E\Pi R}\bar{c}_{11}$	where $\bar{c}_{11} = \int_0^{\bar{d}} \bar{\alpha} F_1^2(\bar{g})\, d\bar{\alpha} \int_0^{\bar{b}} d\bar{z}$
$c_{22} = \dfrac{4\beta_z^2(1-\nu^2)}{E\Pi R}\bar{c}_{22}$	where $\bar{c}_{22} = \int_0^{\bar{d}} \bar{\alpha} F_{II}^2(\bar{g})\, d\bar{\alpha} \int_0^{\bar{b}} d\bar{z}$
$c_{33} = \dfrac{4\beta_y^2(1-\nu^2)}{E\Pi R}\bar{c}_{33}$	where $\bar{c}_{33} = \int_0^{\bar{d}} \bar{\alpha} F_{III}^2(\bar{g})\, d\bar{\alpha} \int_0^{\bar{b}} d\bar{z}$
$c_{44} = \dfrac{16(1-\nu^2)}{E\Pi R^3}\bar{c}_{44}$ $A = \int_0^{\bar{d}} \bar{\alpha} F_{III}^2(\bar{g})\, d\bar{\alpha} \int_0^{\bar{b}} (1-\bar{z}^2) d\bar{z},$	where $\bar{c}_{44} = (1+\nu)A + B$ $B = \int_0^{\bar{d}} \bar{\alpha} F_{II}^2(\bar{g})\, d\bar{\alpha} \int_0^{\bar{b}} \bar{z}^2 d\bar{z}$
$c_{55} = \dfrac{64(1-\nu^2)}{E\Pi R^3}\bar{c}_{55}$	where $\bar{c}_{55} = \int_0^{\bar{d}} \bar{\alpha} F_2^2(\bar{g})\, d\bar{\alpha} \int_0^{\bar{b}} \bar{z}^2 d\bar{z}$
$c_{66} = \dfrac{64(1-\nu^2)}{E\Pi R^3}\bar{c}_{66}$	where $\bar{c}_{66} = \int_0^{\bar{d}} \bar{\alpha} F_1^2(\bar{g})\, d\bar{\alpha} \int_0^{\bar{b}} (1-\bar{z}^2) d\bar{z}$
$c_{15} = \dfrac{16(1-\nu^2)}{E\Pi R^2}\bar{c}_{15}$	where $\bar{c}_{15} = \int_0^{\bar{d}} \bar{\alpha} F_1(\bar{g}) F_2(\bar{g})\, d\bar{\alpha} \int_0^{\bar{b}} \bar{z} d\bar{z}$
$c_{16} = \dfrac{16(1-\nu^2)}{E\Pi R^2}\bar{c}_{16}$	where $\bar{c}_{16} = \int_0^{\bar{d}} \bar{\alpha} F_1^2(\bar{g})\, d\bar{\alpha} \int_0^{\bar{b}} \sqrt{1-\bar{z}^2}\, d\bar{z}$
$c_{56} = \dfrac{64(1-\nu^2)}{E\Pi R^3}\bar{c}_{56}$	where $\bar{c}_{56} = \int_0^{\bar{d}} \bar{\alpha} F_1(\bar{g}) F_2(\bar{g})\, d\bar{\alpha} \int_0^{\bar{b}} \sqrt{1-\bar{z}^2}\, \bar{z} d\bar{z}$
$c_{24} = \dfrac{8\beta_z(1-\nu^2)}{E\Pi R^2}\bar{c}_{24}$	where $\bar{c}_{24} = \int_0^{\bar{d}} \bar{\alpha} F_{II}^2(\bar{g})\, d\bar{\alpha} \int_0^{\bar{b}} \bar{z} d\bar{z}$
$c_{34} = \dfrac{8\beta_y(1+\nu)^2(1-\nu)}{E\Pi R^2}\bar{c}_{34}$	where $\bar{c}_{34} = \int_0^{\bar{d}} \bar{\alpha} F_{III}^2(\bar{g})\, d\bar{\alpha} \int_0^{\bar{b}} \sqrt{1-\bar{z}^2}\, d\bar{z}$

where: $\bar{\alpha} = \alpha/R$, $\bar{d} = d/R$, $\bar{b} = b/R$, $\bar{z} = z/R$, $\bar{g} = \alpha/h$, $d\bar{\alpha} = d\alpha/R$, $d\bar{z} = dz/R$, notations the same as in Fig.2a.

APPENDIX 3

The relations used for calculating the additional flexibility coefficients c_{ij}^{1} (rectangular cross-section, plane state of strain):

$c_{11} = \frac{4\Pi(1-\nu^2)}{EB}\bar{c}_{11}$	where	$\bar{c}_{11} = \int_0^{\bar{a}} \bar{\alpha} F_1^2(\bar{\alpha}) d\bar{\alpha} \int_0^{1/2} d\bar{z}$
$c_{22} = \frac{4\beta_x^2\Pi(1-\nu^2)}{EB}\bar{c}_{22}$	where	$\bar{c}_{22} = \int_0^{\bar{a}} \bar{\alpha} F_{II}^2(\bar{\alpha}) d\bar{\alpha} \int_0^{1/2} d\bar{z}$
$c_{33} = \frac{4\beta_y^2\Pi(1-\nu^2)}{EB}\bar{c}_{33}$	where	$\bar{c}_{33} = \int_0^{\bar{a}} \bar{\alpha} F_{III}^2(\bar{\alpha}) d\bar{\alpha} \int_0^{1/2} d\bar{z}$
$c_{44} = \frac{4\Pi(1-\nu^2)H^2B}{E}\bar{c}_{44}$ $A = \int_0^{\bar{a}} \bar{\alpha}\Phi_z^2 F_{III}^2(\bar{\alpha}) d\bar{\alpha} \int_0^{1/2} d\bar{z}$,	where	$\bar{c}_{44} = (1+\nu)A + B$ $B = \int_0^{\bar{a}} \bar{\alpha}\Phi_y^2 F_{II}^2(\bar{\alpha}) d\bar{\alpha} \int_0^{1/2} d\bar{z}$
$c_{55} = \frac{576\Pi(1-\nu^2)}{EB^3}\bar{c}_{55}$	where	$\bar{c}_{55} = \int_0^{\bar{a}} \bar{\alpha} F_2^2(\bar{\alpha}) d\bar{\alpha} \int_0^{1/2} \bar{z}^2 d\bar{z}$
$c_{66} = \frac{144\Pi(1-\nu^2)}{EBH^2}\bar{c}_{66}$	where	$\bar{c}_{66} = \int_0^{\bar{a}} \bar{\alpha} F_1^2(\bar{\alpha}) d\bar{\alpha} \int_0^{1/2} d\bar{z}$
$c_{15} = \frac{48\Pi(1-\nu^2)}{EB^2}\bar{c}_{15}$	where	$\bar{c}_{15} = \int_0^{\bar{a}} \bar{\alpha} F_1(\bar{\alpha}) F_2(\bar{\alpha}) d\bar{\alpha} \int_0^{1/2} \bar{z} d\bar{z}$
$c_{16} = \frac{24\Pi(1-\nu^2)}{EBH}\bar{c}_{16}$	where	$\bar{c}_{16} = \int_0^{\bar{a}} \bar{\alpha} F_1^2(\bar{\alpha}) d\bar{\alpha} \int_0^{1/2} d\bar{z}$
$c_{56} = \frac{288\Pi(1-\nu^2)}{EHB^2}\bar{c}_{56}$	where	$\bar{c}_{56} = \int_0^{\bar{a}} \bar{\alpha} F_1(\bar{\alpha}) F_2(\bar{\alpha}) d\bar{\alpha} \int_0^{1/2} \bar{z} d\bar{z}$
$c_{24} = \frac{4\beta_x\Pi H(1-\nu^2)}{E}\bar{c}_{24}$	where	$\bar{c}_{24} = \int_0^{\bar{a}} \bar{\alpha}\Phi_y F_{II}^2(\bar{\alpha}) d\bar{\alpha} \int_0^{1/2} d\bar{z}$
$c_{34} = \frac{8\beta_y\Pi H(1+\nu)^2(1-\nu)}{E}\bar{c}_{34}$	where	$\bar{c}_{34} = \int_0^{\bar{a}} \bar{\alpha}\Phi_x F_{III}^2(\bar{\alpha}) d\bar{\alpha} \int_0^{1/2} d\bar{z}$

where: $\bar{z} = z/B$, $\bar{\alpha} = \alpha/H$, $\bar{a} = a/H$, $d\bar{z} = dz/B$, $d\bar{\alpha} = d\alpha/H$, notations as in Fig.2b.

REFERENCES

1. G.R.IRWIN, *Analysis of stresses and strains near the end of a crack traversing a plate*, Trans. ASME, J. of Appl. Mech., **24**, 361-364, 1956.
2. J.WAUER, *On the dynamics of cracked rotors: a literature survey*, Appl. Mech. Rev., **43**, 13-17, 1990.
3. A.D.DIMAROGONAS and C.A. PAPADOPOULOS, *Vibration of cracked shafts in bending*, J. of Sound and Vibr., **91**, 583-593, 1983.
4. C.A.PAPADOPOULOS and A.D.DIMAROGONAS, *Coupled longitudinal and bending vibrations of rotating shaft with an open crack*, J. of Sound and Vibr., **117**, 81-93, 1987.
5. N.ANIFANTIS and A.D.DIMAROGONAS, *Stability of columns with a single crack subjected to follower and vertical loads*, Int. J. of Sol. Struct., **19**, 281-291, 1983.
6. C.A.PAPADOPOULOS, A.D.DIMAROGONAS, *Coupling of bending and torsional vibration of a cracked Timoshenko shaft*, Ing. Archiv., **57**, 495-505 1987.
7. M.D.RAJAB, A.AL-SABEEH, *Vibrational characteristics of cracked shafts*, J. of Sound and Vibr., **147**, 465-173, 1991.
8. W.OSTACHOWICZ, M.KRAWCZUK, *Analysis of the effect of cracks on the natural frequencies of a cantilever beam*, J. of Sound and Vibr., **150**, 191-201, 1991.
9. S.CHRISTIDIS and A.D.S. BARR, *One-dimensional theory of cracked Bernoulli-Euler beams*, Int. J. of Mech. Sci., **26**, 639-648, 1984.
10. T.A.HENRY and B.E.OKAH-AVAE, *Vibrations in cracked shafts*, IME London, Vibration of Rotating Machinery, 15-19, 1976.
11. H.OKAMURA, W.W.LIU, C-S.CHU and H.LIEBOWITZ, *A cracked column under compression*, Eng. Fract. Mech., **1**, 547-564, 1969.
12. I.W.MAYES and W.G.R.DAVIES, *The vibrational behaviour of a rotating shaft system containing a transverse crack*, IME London, Vibration of Rotating Machinery, 53-65, 1976.
13. B.O. DIRR and B.K.SCHMALHORST, *Crack depth analysis of a rotating shaft by vibration measurement*, Proc, of 11-th Biennial Conference on Mechanical Vibration and Noise, **2**, 607-614, 1987.
14. W.OSTACHOWICZ and M.KRAWCZUK, *Vibration analysis of a cracked beam*, Comp. and Struct., **36**, 245-250, 1990.
15. W.OSTACHOWICZ and M.KRAWCZUK, *Vibration analysis of cracked turbine and compressor blades*, ASME 35-th International Gas Turbine and Aeroengine Congress and Exposition, 90-GT-5, 1990.
16. M.H.H.SHEN and C.PIERRE, *Natural modes of Bernoulli-Euler beams with symmetric cracks*, J. of Sound and Vibr., **138**, 115-134, 1990.
17. B.S.HAISTY and W.T.SPRINGER, *A general beam element for use in damage assessment of complex structures*, Trans. ASME, J. of Vibr., Acoust. Stress and Rel. in Design, **110**, 389-394, 1988.

18. G.L.QIAN, S.N.GU and J.S.JIANG, *The dynamic behaviour and crack detection of a beam with crack*, J. of Sound and Vibr., **138**, 233-243, 1990.

19. G. GOUNARIS and A.D.DIMAROGONAS, *A finite element of a cracked prismatic beam for structural analysis*, Comp. and Struct., **28**, 309-313, 1988.

20. G.L.QIAN, S.N.GU and J.S.JIANG, *A finite element model of cracked plates and application to vibration problems*, Comp. and Struct., **39**, 483-487, 1991.

21. G.R. COWPER, *The shear coefficient in Timoshenko's beam theory*, Trans. ASME, J. of Appl. Mech., 335-340, 1966.

22. J.F.KNOTT, *Fundamentals of fracture mechanics*, Butterworths, London 1973.

23. J.S.PRZEMIENIECKI, *Theory of matrix structural analysis*, Mc Graw-Hill, New York 1968.

24. M.KRAWCZUK, *Dynamics of one-dimensional media with materials faults*, [in Polish], Doctoral Thesis, IFFM-PAS, Gdańsk 1991.

25. T.HUBER, *Elasticity theory*, [in Polish], WNT, Warszawa 1956.

26. O.C.ZIENKIEWICZ, *The Finite Element Method in Engineering*, [Polish trans.], Arkady, Warszawa 1972.

27. IBM *Application program*, Techn. Publ. Depart., New York 1970.

INSTITUTE OF FLUID FLOW MACHINERY PAS.

Received October 21,1991.